Analytica Chimica Acta 902 (2016) 182–188

Contents lists available at ScienceDirect

Analytica Chimica Acta

journal homepage: www.elsevier.com/locate/aca

Molecularly imprinted polymer film interfaced with Surface Acoustic Wave technology as a sensing platform for label-free protein detection

Aleksei Tretjakov, Vitali Syritski*, Jekaterina Reut, Roman Borozniak, Andres Öpik

Department of Materials Science, Tallinn University of Technology, Ehitajate tee 5, 19086 Tallinn Estonia

HIGHLIGHTS

- A facile integration of protein-MIPs with SAW technology was firstly reported.
- IgG-MIP ultrathin films were interfaced with the multiplexed SAW chips by an electrosynthesis approach.
- The selectivity of IgG-MIP films toward IgG over IgA and HSA was demonstrated.

GRAPHICAL ABSTRACT

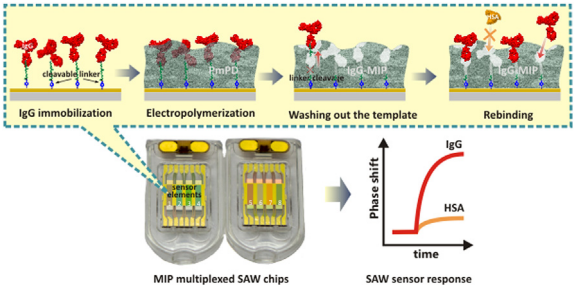

ARTICLE INFO

Article history:
Received 18 July 2015
Received in revised form 29 October 2015
Accepted 4 November 2015
Available online 17 November 2015

Keywords:
Molecularly imprinted polymer
Electrochemical polymerization
Immunoglobulin G
Surface acoustic wave

ABSTRACT

Molecularly imprinted polymer (MIP)-based synthetic receptors integrated with Surface Acoustic Wave (SAW) sensing platform were applied for the first time for label-free protein detection. The ultrathin polymeric films with surface imprints of immunoglobulin G (IgG-MIP) were fabricated onto the multiplexed SAW chips using an electrosynthesis approach. The films were characterized by analyzing the binding kinetics recorded by SAW system. It was revealed that the capability of IgG-MIP to specifically recognize the target protein was greatly influenced by the polymer film thickness that could be easily optimized by the amount of the electrical charge consumed during the electrodeposition. The thickness-optimized IgG-MIPs demonstrated imprinting factors towards IgG in the range of 2.8–4, while their recognition efficiencies were about 4 and 10 times lower toward the interfering proteins, IgA and HSA, respectively. Additionally, IgG-MIP preserved its capability to recognize selectively the template after up to four regeneration cycles. The presented approach of the facile integration of the protein-MIP sensing layer with SAW technology allowed observing the real-time binding events of the target protein at relevant sensitivity levels and can be potentially suitable for cost effective fabrication of a biosensor for analysis of biological samples in multiplexed manner.

1. Introduction

Today label-free detection of proteins has become of extensive demand in fundamental research as well as in clinical practice providing an alternative to the widely used label-based detection methods that involves laborious, lengthy procedure and can influence the interfacial activity of the resulting protein–label complexes, and consequently the accuracy of measurement results [1]. Label-free detection can be implemented with the help of various transduction mechanisms, including, but not limited to, optical, electrochemical or piezoelectric, where the biochemical interaction between an analyte and a recognition element of the sensor

* Corresponding author.
E-mail address: vitali.syritski@ttu.ee (V. Syritski).

http://dx.doi.org/10.1016/j.aca.2015.11.004
0003-2670/

is recorded as a change in e.g., refractive index (SPR sensors), impedance (electrochemical sensors) or resonance frequency (QCM sensors), respectively.

Common recognition elements in biosensors are biomacromolecules such as antibodies, enzymes, or DNA, that can capture target analyte with very high affinity and specificity. However, due to the restricted operating conditions and high production cost of these biological receptors, the development of artificial systems with molecular recognition capability, so-called synthetic receptors, have gained a lot of interest as potential alternatives for biological recognition elements. Among a number of existing techniques for design of synthetic receptors, high expectations are set in the development of molecularly imprinted polymers (MIPs). The technique of molecular imprinting allows the formation of specific molecular recognition sites in highly reticulated polymeric network grown in the present of analyte molecules, which are subsequently removed leaving behind the analyte specific cavities. MIPs have been shown to possess several advantages as an alternative recognition material for biosensor including low cost, the ease of preparation, storage stability, repeated operations without loss of activity, high mechanical strength, durability to heat and pressure, as well as applicability in harsh chemical media [2,3].

Although synthesis of MIP materials recognizing small molecular weight compounds has proven to be very successful, molecular imprinting of biomacromolecules, in particular proteins, obviously has encountered challenges due their inherent properties such as molecular size, complexity, conformational flexibility, and solubility [4]. Thus, the hindered mass transfer of a large biomolecule in highly reticulated polymeric networks prepared by conventional bulk imprinting leads to their entrapment during imprinting rather than to binding sites permitting free ligand exchange with the sample solution. A number of imprinting strategies were elaborated in order to address the issues associated with protein imprinting [4,5]. The surface imprinting approach leading to the formation of polymer with imprinted sites located at or close to the surface of MIPs, enabling easy access to the target macromolecules, was shown to be a promising way for protein-MIP preparation [6–8].

Many of the reported surface imprinting strategies take advantage of the facile integration of protein-MIP sensing layer with a transducer that is a key aspect in the design of a MIP-based sensor. Thus, the microcontact surface imprinting approach based on photopolymerization has been widely studied to prepare a surface imprinted polymer thin film directly on the surface for selective recognition of C-reactive protein [6], trypsin [9], bovine serum albumin [10]. In another surface imprinting approach, the sol–gel method was combined with a self-assembly technology to prepare a human serum albumin (HSA)-imprinted film on the surface of a QCM [11]. Electrosynthesis has been introduced recently as a convenient strategy for effectively interfacing protein-MIPs with transducers allowing rapid and controlled deposition of polymer films with tunable thickness [7,12–17]. It is worth to mention that in the most of the reported works using protein-MIPs for sensing applications QCM, SPR or electrochemical sensors are preferential choice. Meanwhile, Surface Acoustic Waves (SAW) may provide advances in fabrication of MIP-based sensors over these technologies. Generally, SAW devices share the similar principle of operation as QCMs, but utilize acoustic waves at surfaces rather than in the bulk of a piezoelectric material allowing to increase operating frequencies of SAW devices to the range of 100–500 MHz without compromising in their mechanical fragility. The Love Wave sensor, a special class of the shear-horizontal SAW having the acoustic energy propagation path strictly confined inside of the guiding layer coated onto the top of the sensor. This layer minimizes the energy dissipation losses into environmental media making thus the Love Wave sensors, besides their extremely high sensitivity towards surface effects, well suited for operation in liquids. Usually, owing to high operation frequencies SAW offers about an order of magnitude higher mass resolution than QCMs, while keeps sensor cost low and at the same time is fully compatible with large-scale fabrication and multiplexing technologies [18,19]. As compared to SPR, SAW technology is not limited to detect only mass loading onto the surface, but also useful to follow structural insights of sensing layers through use of dissipation factor of the acoustic wave propagating along the sensor surface.

Despite of the mentioned advantages, integration of SAW sensors with polymeric synthetic receptor materials has not yet been sufficiently displayed. While SAW gas sensors with a MIP-based recognition layer have been reported [20,21], there is no a report, however, on a sensor of similar type designed for protein selective recognition. To fill this void, here we have integrated the IgG-MIPs with SAW technology by facile electrochemical synthesis approach. The special attention was paid to the careful choice of optimal polymer thickness to prepare IgG-MIP with the improved recognition properties. The binding kinetics were analyzed to differentiate the equilibrium binding capacities and affinities of the targets to IgG-MIP and NIP surfaces. The regeneration, and thus reusability of the IgG-MIP-modified SAW chips after the repeated regeneration cycles was also examined.

2. Experimental

2.1. Chemicals and materials

IgG from human serum, IgA from human serum, HSA from human serum, 4-aminothiophenol (4-ATP), *m*-phenylenediamine (mPD), 2-mercaptoethanol, phosphate buffer saline (PBS) tablets, sodium chloride were obtained from Sigma–Aldrich. 3,3′-dithiobis[sulfosuccinimidylpropionate] (DTSSP) was purchased from ThermoFisher Scientific Inc. All chemicals were of analytical grade or higher and were used as received without any further purification. Ultrapure water (resistivity 18.2 MΩ cm, Millipore, USA) was used for preparation of all aqueous solutions. Phosphate buffered saline (PBS) solution (0.01 M, pH 7.4) was used to prepare synthesis and analyte solutions.

2.2. IgG-MIP film preparation

IgG-MIP films were fabricated directly on Love Wave-configured SAW chips (NanoTemper Technologies GmbH, München, Germany) according to the previously developed procedure (Fig. 1) [14]. The procedure was undergone some modifications with intention to improve analytical performance of the resulting films. In brief, the gold sensing surface of SAW chip consisting of four sensor elements was preliminary cleaned by a fresh base piranha solution (25% NH_4OH:30% H_2O_2:H_2O, 1:1:5 volume ratio) for 15 min, rinsed abundantly with ultrapure water, and treated in an UV/ozone cleaner followed by rinsing with ultrapure water and drying in a nitrogen stream. Then, IgG was immobilized on the cleaned surface through DTSSP cleavable crosslinker. For this purpose, the surface was functionalized with amino-groups by immersion in the ethanolic solution of 0.1 M 4-ATP for 1 h and then, DTSSP crosslinker was covalently attached by incubation in PBS buffer (pH 7.4) containing 10 mM of DTSSP for 30 min. After that, 0.1 mL of PBS containing 1 mg mL^{-1} of IgG was dropped onto the modified sensing surface and allowed to react for 30 min, followed by additional rinsing with PBS buffer to remove the unbound IgG. The protein-modified SAW chip was placed into the 5-mL electrochemical cell designed to expose the modified sensing surface to the synthesis solution. The electrochemical cell accommodated

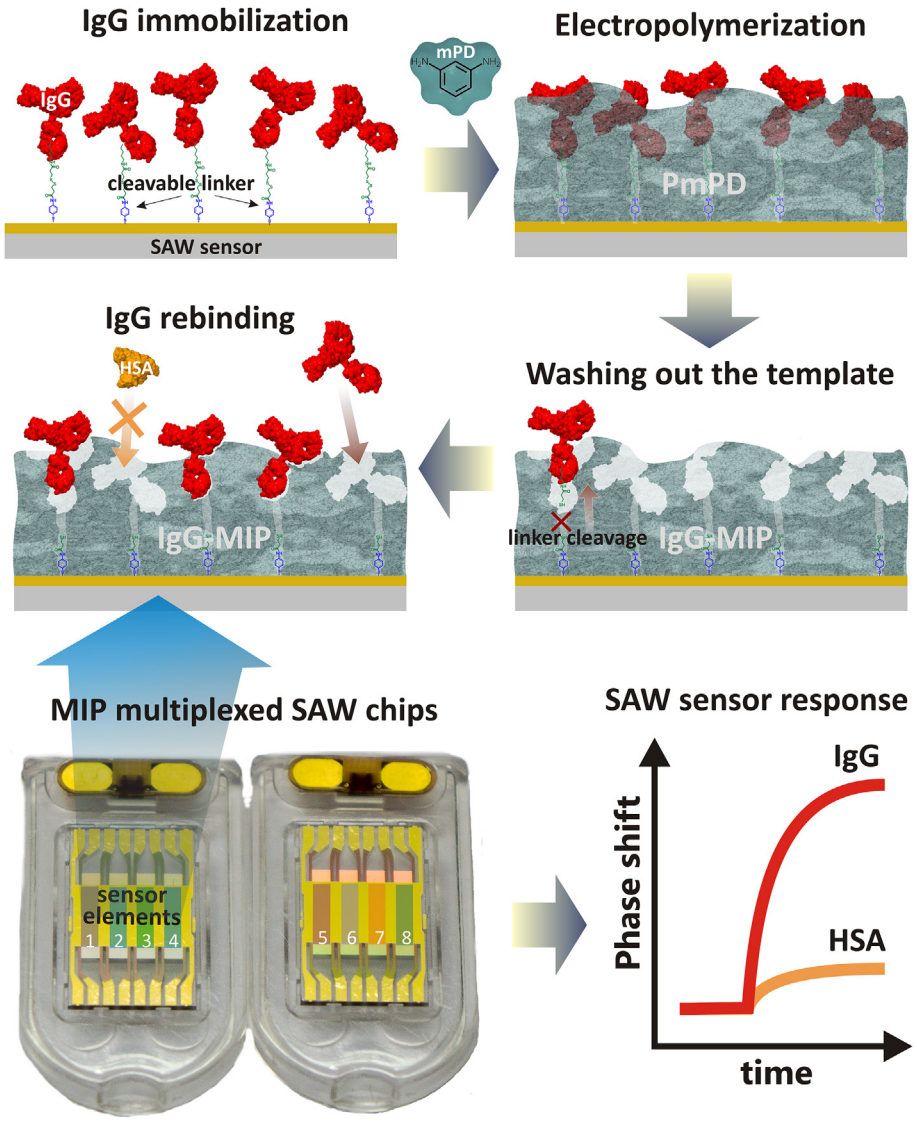

Fig. 1. Schematic representation of the synthesis concept for IgG-MIP sensing layer integration with SAW chip.

three electrodes, i.e. the sensing surface of SAW chip as a working electrode, a spiral shaped Pt wire as a counter electrode, and Ag/AgCl/KCl_{sat} as a reference electrode, all connected to an electrochemical workstation (Reference 600™, Gamry Instruments, Inc., USA). *m*-PD electropolymerization on the IgG-modified surface was carried out in PBS buffer solution containing 10 mM of mPD by imposing the constant potential of 0.9 V to the working electrode.

To yield the polymeric structures of defined thickness their growth were controlled by charge passed through the working electrode. Thicknesses were determined by a spectroscopic ellipsometer (SE 850 DUV, Sentech Instruments GmbH, Berlin, Germany). Ellipsometric parameters ψ and Δ were measured from three spots for each sample in ambient air confining the wavelength range between 380 and 850 nm at the angle of incidence of 70°. The spectra were fitted (SpectraRay 3 software) with the optical model containing a one-layer Cauchy layer on the top of the gold and the thicknesses were determined.

After the electrodeposition the PmPD film coated sensing surface was rinsed with ultrapure water and dried in a nitrogen stream. To remove the template protein, IgG, from the electrodeposited PmPD film the modified sensing surface was immersed in aqueous solution of 0.1 M 2-mercaptoethanol, and heated in water bath up to 100 °C with stirring for 15 min. After that, the sensing surface was washed additionally in 3 M NaCl aqueous solution for 15 min and in DMSO for 30 min. The resulting IgG-MIP SAW chip was washed thoroughly with ultrapure water and subjected to the protein rebinding studies. To assess the IgG-MIPs in terms of their affinity to IgG molecule, control non-imprinted polymer (NIP) structures were also created using the very same conditions as for the IgG-MIP but excluding the linker cleavage stage by mercaptoethanol. In this case, the NIP films still contained the covalently bound target protein, but had no specific cavities on its surface.

2.3. IgG rebinding studies

Real-time rebinding of IgG on the prepared IgG-MIP-modified SAW chips was performed using a SAW biosensor system (SamX®, NanoTemper Technologies GmbH, München, Germany) capable to handle two SAW chips having four separate sensor elements each. The microfluidics of the system provided the option to deliver

analyte solutions to the modified sensor elements either individually or in serial fashion.

The sensor elements were preconditioned at constant flow (25 μL min^{-1}) of the degassed PBS buffer solution (pH = 7.4) until a constant baseline was reached. Subsequently, various concentrations (from 0.4 nM to 53 nM) of analytes prepared from the same buffer were injected into the flow stream via an autosampler using a 430 μL injection loop and allowed to interact with the IgG-MIP or IgG-NIP modified SAW chip.

The SAW sensor system capable of both phase and amplitude signal measurement, reflecting changes in mass and in viscoelastic properties of a material at the sensor surface, respectively. In this work, phase-shift response was analyzed to evaluate rebinding properties of IgG-MIPs. Data analysis was performed using Origin 9.1 (Northampton, MA). Raw data were exported, cut and analyzed by individual fits using two kinetic models for sorption from liquid solution represented by the first- and second-order equations as described in the Results and Discussion section. Affinity constants and K_D values were determined from plot of the equilibrium signal (Q_{eq}) versus analyte concentration using Langmuir–Freundlich equation for the data fitting. Regeneration of the film-modified chips was done by their immersion in 3 M NaCl aqueous solution for 2 h with stirring and heating up to 100 °C.

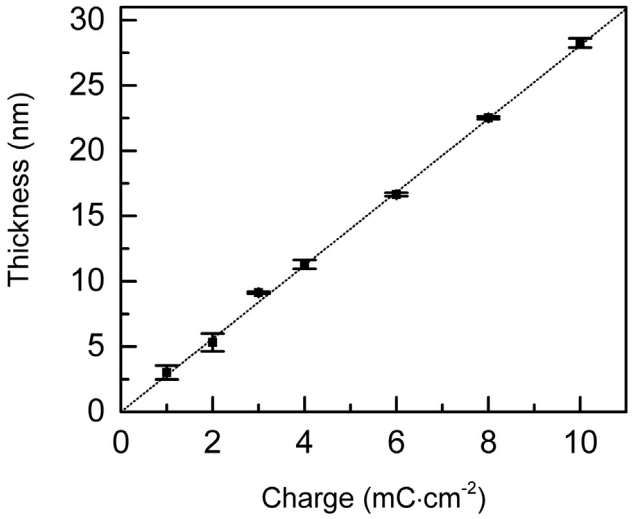

Fig. 2. The calibration graph representing the dependence of the polymeric film thickness, as measured by the spectroscopic ellipsometry, on the amount of the charge consumed during the electropolymerization of *m*-PD on IgG-modified gold electrode.

3. Results and discussion

3.1. IgG-MIP fabrication

In contrast to the previously reported synthesis strategy [14], some modifications were introduced here in order to improve the selectivity of the resulting IgG-MIPs. mPD was used as a functional monomer for polymer matrix formation instead of dopamine. Electropolymerization of mPD proceeds faster than that of dopamine therefore the surface-immobilized IgG is less exposed to the synthesis solution as well as to the applied potential that significantly reduces the possibility of conformational changes of IgG. In addition, the computational modeling using molecular docking and quantum chemical approach revealed that mPD as a functional monomer minimally affected the conformation of IgG and was able to create molecular memory via multiple hydrogen bonds, van der Waal's and lipophilic interactions between the polymer matrix and IgG [22]. Moreover, taking into account the types of possible interactions between PmPD and IgG, the template washing out procedure was also modified by including the treatment with 3 M NaCl solution and DMSO in addition to the cleavage of DTSSP linker with mercaptoethanol.

The electrosynthesis approach to the preparation of MIP films allowed a fine control of the polymer thickness by monitoring the electrical charge passed during the synthesis. For the surface imprinting strategy used in this study the deposition of a polymer film with an appropriate thickness is one of the most important task in order to produce protein-MIP film with specific binding sites located on the surface [23,24]. The influence of the electrodeposited polymer thickness on the specific recognition properties of IgG-MIP has been already demonstrated in the previous study [14]. Thereby, in this study to avoid irreversible entrapment of the template the special attention was paid to the careful choice of optimal polymer thickness through control of the charge passed during the in-situ electrodeposition and subsequent correlation of the data with the *ex-situ* ellipsometry measurements (Fig. 2). As it can be seen, the deposited polymer thickness varied nearly linearly (R^2 = 0.996) across the applied electric charge range making thus its prediction between ca. 3 nm and 30 nm quite certain. Since the height of IgG with the immobilizing linker system above the surface may spread from ca. 10.5 till 20 nm [14] PmPD films with the thicknesses in the range of 5.7 nm and 28.4 nm were synthesized on the IgG-modified SAW chips by applying the respective charge between 2 and 10 mC cm^{-2}. The influence of the polymer film thickness on IgG-MIP capability to specifically recognize the target protein was evaluated in the course of IgG rebinding study as discussed below.

3.2. IgG rebinding study

The fabricated IgG-MIPs were characterized in term of their affinity to IgG by monitoring the binding kinetics with SAW system. Typical sensorgrams of IgG rebinding at the different concentrations to the surface of SAW chip modified with 11 nm thick IgG-MIP and NIP are presented in Fig. 3a. The association phase of the sensorgrams was analyzed in order to determine the equilibrium signal for the IgG to IgG-MIP and NIP surfaces by fitting the response to the pseudo-first order and pseudo second order kinetic Eqs. (1) and (2), respectively:

$$Q = Q_{eq}\left[1 - e^{-k_1 * t}\right] \quad (1)$$

$$Q = \left[Q_{eq}^2 k_2 t\right]/[1 + Q_{eq} k_2 t] \quad (2)$$

where Q is the phase-shift response upon IgG rebinding at time t, Q_{eq} is its value at equilibrium, k_1 is a pseudo-first order rate constant, k_2 is a pseudo-second order rate constant. The first and second order rate models have been widely used to describe adsorption data obtained under non-equilibrium conditions [25]. According to the first order kinetics model, the adsorbate binds only to a single active site on the adsorbent surface and the interactions of adsorbate and adsorbent are of physical nature; the rate of occupation of adsorption sites is proportional to the number of unoccupied sites [26,27]. The pseudo-second order model recognizes that the rate-limiting step is chemisorption involving sharing or exchange of electrons between adsorbent and adsorbate and the rate of occupation of adsorption sites is proportional to the square of the number of unoccupied sites [27,28]. Both models have been applied to describe the adsorption kinetics on the MIP surfaces [29–31].

The kinetics parameters obtained by fitting the sensorgrams in Fig. 3a to the Eqs. (1) and (2) are listed in the Table 1. As it can be seen both models provided excellent fit to the experimental data with the correlation coefficients (R^2) in the range of

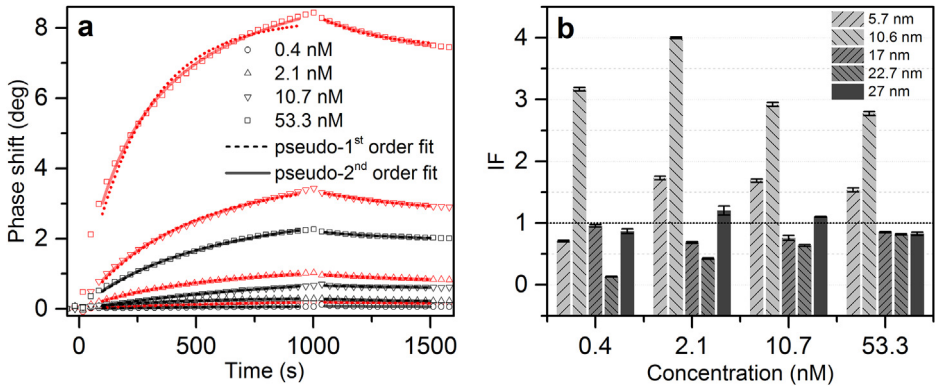

Fig. 3. (a) Typical phase-shift responses of the IgG-MIP (red) and NIP (black) modified SAW chips (PmPD film thickness of 11 nm) upon consecutive injections of IgG in PBS buffer. The dotted and solid lines represent the fits to the Eq. (1) and Eq. (2), respectively; (b) The calculated *IF* values for IgG-MIPs prepared with PmPD films of different thicknesses as a function of the IgG concentration. (For interpretation of the references to color in this figure legend, the reader is referred to the web version of this article.)

Table 1
The kinetics parameters obtained by fitting the sensorgrams in Fig. 3a to the pseudo-first order and pseudo-second order kinetic models.

C (nM)	Q_{eq} (MIP) (deg)	k[a]	R^2	Q_{eq}(NIP) (deg)	k[a]	R^2
Pseudo-first order model						
0.4	0.24	1.51E-03	0.994	0.08	1.83E-03	0.965
2.1	1.13	2.15E-03	0.998	0.30	3.01E-03	0.994
10.7	3.65	2.37E-03	0.994	1.06	9.90E-04	0.999
53.3	8.25	3.98E-03	0.978	2.58	2.09E-03	0.997
Pseudo-second order model						
0.4	0.38	2.72E-03	0.995	0.12	1.15E-02	0.965
2.1	1.64	1.00E-03	0.999	0.41	6.18E-03	0.995
10.7	5.17	3.66E-04	0.999	1.77	3.43E-04	0.999
53.3	10.43	3.90E-04	0.997	3.76	4.21E-04	0.999

[a] Pseudo-first order rate constant (s^{-1}) or pseudo-second order rate constant (deg^{-1} s^{-1}).

0.965–0.999, although, at the higher analyte concentrations, somewhat higher values were obtained for the second order adsorption model. The latter might be explained by the fact that Q_{eq} in the pseudo-second order model can be determined independently of the kinetic mechanism of the adsorption process [32] and is less prone to the random experimental errors as compared to the first order rate equation [27]. Thus, Q_{eq} values determined by the pseudo-second rate model were used further to assess the degree of recognition capability of MIP towards the target molecule calculating imprinting factor (*IF*). Actually, *IF* shows a binding ratio between MIP and NIP:

$$IF = Q_{eq}(MIP)/Q_{eq}(NIP) \quad (3)$$

where Q_{eq} *(MIP)* and Q_{eq} *(NIP)* are phase-shift responses at equilibrium for MIP and NIP, respectively. As a measure of the presence of selective cavities, *IF* was taken into account to optimize the thickness of the PmPD film in IgG-MIP. SAW chips modified with IgG-MIP and NIP of different thicknesses in the range of ca 6 and 27 nm were subjected to interact with various IgG concentrations between 0.4 and 53.3 nM. Fig. 3b clearly indicates that for all IgG concentrations studied the highest *IF* values in the range of 2.8–4.0 were obtained for the IgG-MIP with PmPD film of 11 nm. This polymer thickness corresponds to the half of the height of immobilized IgG that was estimated to be around 20 nm assuming the IgG "end-on" orientation (through the Fc region). Obviously, at such polymer film thickness the immobilized IgG molecules might be appropriately confined in the polymer leading to the increasing number of high-affinity binding sites at the polymer surface after the IgG removal procedure. Thus, the thickness-optimized IgG-MIP films were employed for subsequent analysis of equilibrium parameters, regeneration and selectivity studies.

Adsorption isotherms are of particular interest as they represent the dependence of the equilibrium concentration of a bound analyte on the concentration of a free analyte in a solution and can provide useful information on the binding properties of the material by fitting the isotherm to specific binding models. The isotherm of IgG rebinding to IgG-MIP was constructed using the values of Q_{eq} determined from analysis of the experimental kinetic data fitting them to Eq. (2) (Fig. 4). Considering the binding site heterogeneity was frequently encountered in noncovalent MIPs [33] the analyte rebinding was modeled by the Langmuir–Freundlich (LF) isotherm (Eq. (4)).

$$Q = Q_{max}C^m/(K_D + C^m) \quad (4)$$

Here *C* is the concentration of an analyte in a solution, *Q* and Q_{max} the phase-shift responses upon IgG rebinding at concentration *C* and its saturation value, respectively, *m* is the heterogeneity index, which varies from 0 to 1 and with values < 1, the material is heterogeneous, K_D – equilibrium dissociation constant. According to Fig. 4 LF model gives an excellent fit ($R^2 = 0.999$) for both IgG-MIP and NIP films tested in this study. The calculated *m* value of IgG-MIP indicates the somewhat heterogeneity of the binding sites in comparison to NIP, whose heterogeneity index equals to 1 corresponding to a homogeneous material. This can be well explained through assumption that NIP films might possess the exclusively nonspecific binding sites of equal adsorption energy, while the imprinting process introduced the binding sites with varying degrees of affinity resulting in the heterogeneity of the polymer surface. Furthermore, the obtained value of the signal at saturated binding to IgG-MIP was about 3 times higher than that to corresponding NIP (15.0 vs 5.3 deg) while the only modest difference in the dissociation constants (K_D) between two polymers was observed. One possible explanation for the observed phenomenon could be that despite of the total number of binding sites was increased in MIP relative to the NIP, the fraction of the higher-affinity binding sites was still low to contribute significantly to the overall affinity of IgG-MIP. Similarly, Shimizu and coworkers reported on the inconsistency between the difference in binding capacities and binding affinities of MIP and corresponding NIP [34].

3.3. Regeneration of IgG-MIPs

In order to verify the stability and reusability of the fabricated IgG-MIPs, the films with the optimal thickness after first IgG rebinding were subjected to the regeneration procedure. Since the nature of the interactions between the imprinted material and the target protein was insufficiently known, the regeneration

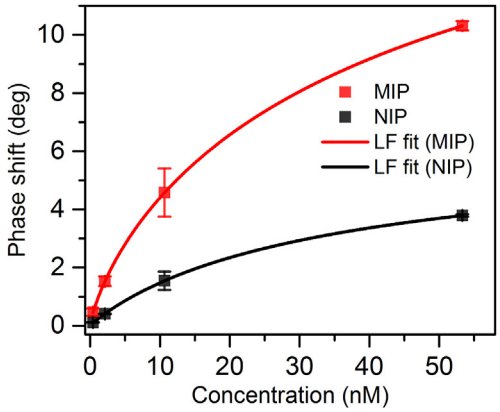

The LF model fitted binding parameters

	MIP	NIP
Q_{max} (deg)	15.0 ± 0.5	5.3 ± 0.5
K_D (nM)	16.5 ± 0.5	21.7 ± 2.4
m	0.91	1
R^2	0.999	0.999

Fig. 4. The binding isotherms obtained using Q_{eq} determined from fitting of the kinetic data to Eq. (2). The solid lines represent fits of the data to Langmuir–Freundlich (LF) isotherm model. The table summarizes the fitted binding parameters.

experiments disrupting hydrogen, ionic and electrostatic bonds were performed. It was found that solutions of 1 M NaOH and 10 mM HCl affected significantly on reproducibility of further binding events making difference between MIP and NIP films barely noticed (results are not shown), while MIPs retained their affinity towards the target after the treatment in 3 M NaCl solution (100 °C) suggesting that electrostatic interactions might play a role in the given MIP-protein system. Therefore, the treatment in the hot 3 M NaCl solution was chosen as a method for regeneration of the fabricated IgG-MIPs. The changes in Q_{max} of the polymers for IgG after the subsequent rebinding-regeneration cycles are depicted in Fig. 5 . As it can be seen, although both MIP and NIP polymers showed irreversible adsorption of the target, their rebinding capacities were about to stabilize after the 3rd regeneration cycle while still demonstrating MIP preferential affinity and relevant sensitivity levels towards the target. The noticed decrease in the adsorption capacity may indicate that the regeneration method left behind to some extent the target entrapped in the polymeric matrix altering thus the following rebinding. Still, the phenomenon cannot be explained purely by the target entrapment since the nonspecific adsorption, displayed by NIP film response, was suppressed significantly after the very 1st regeneration cycle. Thus, the films might also undergo morphological changes upon contact with the high temperature and ionic strength solutions resulting in loss of a fraction of the polymeric material from the sensing surface.

3.4. Selectivity study

Selectivity of IgG imprinted films towards the template was studied by injecting 8 μg mL^{-1} solutions of other serum proteins: HSA and IgA that may cause serious interference when analyzing real samples. Selectivity factor *S*, which is the ratio of *IF* of an interfering substance to that toward the template molecule, was used to assess cross-reactivity of IgG-MIP:

$$S = IF_{(interf)}/IF_{(IgG)} \quad (5)$$

where $IF_{(IgG)}$ is the imprinting factor of IgG-MIP for IgG and $IF_{(interf)}$ is the imprinting factor of IgG-MIP for interfering protein, IgA or HSA. $IF_{(interf)}$ values for IgA and HSA were calculated according to Eq. (3), where the values of Q_{eq} upon HSA and IgA adsorption onto IgG-MIP and NIP were determined from the kinetics data using the similar analysis procedure as described for IgG rebinding study (Section 3.2). As it can be seen in Fig. 6, IgG-MIP demonstrated the preferential binding to the original template molecule (IgG) over the IgA and HSA with the *S* values of 0.3 and 0.09, respectively. The data suggests that the both interfering proteins have lower binding affinity to IgG-MIP than IgG, even though the molecular size and shape of IgG and IgA are similar. Thus, IgG-MIP can recognize the

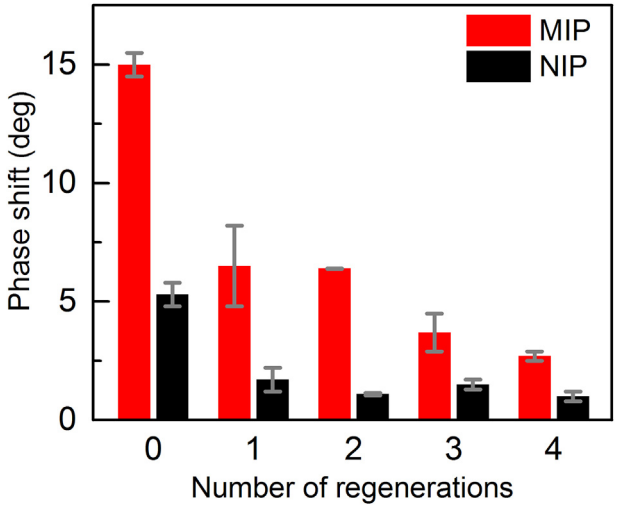

Fig. 5. SAW sensor response at saturated binding (Q_{max}) for IgG-MIP and NIP after various number of regeneration cycles. The initial responses of freshly fabricated sensors are presented at 0 value of regeneration cycle.

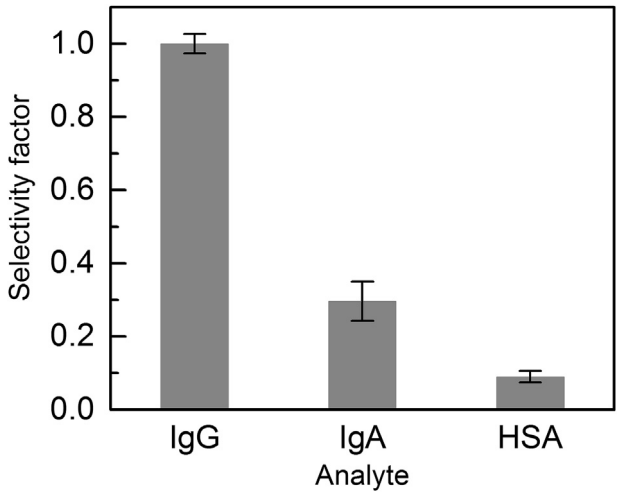

Fig. 6. Selectivity factors (*S*) of IgG-MIP for the template (IgG) and non-template (IgA, HSA) proteins.

target protein confirming the presence of IgG imprints in the polymer matrix that are able to discriminate on the basis of molecular shape and size as well as functional groups arrangement.

4. Conclusions

In this study, the protein imprinted polymers, IgG-MIPs, were used for the first time as sensing layers of SAW sensor platform. The thin films of IgG-MIP were successfully interfaced with SAW chips using the electrosynthesis approach. The binding kinetic analysis with the pseudo second-order rate model allowed the determination of equilibrium binding response and thus, the calculation and comparison of the imprinting factors for the IgG-MIP of different polymer thicknesses. It was found that IgG-MIP films with the thickness of 11 nm had higher specific recognition ability towards IgG as compared to the other studied IgG-MIP counterparts. The thickness optimized MIPs demonstrated imprinting factors in the range of 2.8–4.

The analysis of the isotherm data by fitting them to Langmuir–Freundlich adsorption model suggested a certain degree of heterogeneity of the binding sites in IgG-MIP films. Although, the binding capacity of IgG-MIP was about 3 times higher than that of NIP, their dissociation constants were somewhat comparable. This is more likely attributed to the disproportionately low contribution of the high affinity binding sites to the increased binding capacity of IgG-MIP. The prepared IgG-MIPs demonstrated good selectivity towards IgG over the interfering proteins such as IgA and HSA as well preserved their capability to recognize selectively the template after up to four regeneration cycles in hot 3 M NaCl solution.

The realized concept for facile integration of protein-MIPs with SAW technology allowed observing the real-time binding events of the target protein at relevant sensitivity levels and can be potentially suitable for cost effective fabrication of a biosensor for analysis of biological samples in multiplexed manner.

Acknowledgments

This work was supported by the Estonian Ministry of Education and Research (grant PUT150). The authors thank Dr. J. Rappich for the opportunity to perform the ellipsometry measurements at Helmholtz-Zentrum Berlin für Materialien und Energie GmbH.

References

[1] S. Ray, G. Mehta, S. Srivastava, Label-free detection techniques for protein microarrays: prospects, merits and challenges, Proteomics 10 (2010) 731–748.
[2] S. Li, Y. Ge, S.A. Piletsky, J. Lunec, Molecularly Imprinted Sensors: Overview and Applications, Elsevier, 2012, p. 388.
[3] L. Ye, K. Haupt, Molecularly imprinted polymers as antibody and receptor mimics for assays, sensors and drug discovery, Anal. Bioanal. Chem. 378 (2004) 1887–1897.
[4] N.W. Turner, C.W. Jeans, K.R. Brain, C.J. Allender, V. Hlady, D.W. Britt, From 3D to 2D: A review of the molecular imprinting of proteins, Biotechnol. Prog. 22 (2006) 1474–1489.
[5] H. Nishino, C.S. Huang, K.J. Shea, Selective protein capture by epitope imprinting, Angew. Chem. Int. Ed. 45 (2006) 2392–2396.
[6] P.C. Chou, J. Rick, T.C. Chou, C-reactive protein thin-film molecularly imprinted polymers formed using a micro-contact approach, Anal. Chim. Acta 542 (2005) 20–25.
[7] G. Lautner, J. Kaev, J. Reut, A. Öpik, J. Rappich, V. Syritski, R.E. Gyurcsanyi, Selective Artificial receptors based on micropatterned surface-imprinted polymers for label-free detection of proteins by SPR imaging, Adv. Funct. Mater. 21 (2011) 591–597.
[8] A. Menaker, V. Syritski, J. Reut, A. Öpik, V. Horvath, R.E. Gyurcsanyi, Electrosynthesized surface-imprinted conducting polymer microrods for selective protein recognition, Adv. Mater 21 (2009) 2271–2275.
[9] O. Hayden, C. Haderspock, S. Krassnig, X.H. Chen, F.L. Dickert, Surface imprinting strategies for the detection of trypsin, Analyst 131 (2006) 1044–1050.
[10] D.R. Kryscio, N.A. Peppas, Surface imprinted thin polymer film systems with selective recognition for bovine serum albumin, Anal. Chim. Acta 718 (2012) 109–115.
[11] Z.H. Zhang, Y.M. Long, L.H. Nie, S.Z. Yao, Molecularly imprinted thin film self-assembled on piezoelectric quartz crystal surface by the sol-gel process for protein recognition, Biosens. Bioelectron. 21 (2006) 1244–1251.
[12] J. Rick, T.C. Chou, Using protein templates to direct the formation of thin-film polymer surfaces, Biosens. Bioelectron. 22 (2006) 544–549.
[13] P.S. Sharma, A. Pietrzyk-Le, F. D'Souza, W. Kutner, Electrochemically synthesized polymers in molecular imprinting for chemical sensing, Anal. Bioanal. Chem. 402 (2012) 3177–3204.
[14] A.S. Tretjakov, V. Syritski, J. Reut, O. Volobujeva, A. Öpik, Surface molecularly imprinted polydopamine films for recognition of immunoglobulin G, Microchim. Acta 180 (2013) 1433–1442.
[15] J. Bognar, J. Szucs, Z. Dorko, V. Horvath, R.E. Gyurcsanyi, Nanosphere lithography as a versatile method to generate surface-imprinted polymer films for selective protein recognition, Adv. Funct. Mater 23 (2013) 4703–4709.
[16] D. Cai, L. Ren, H.Z. Zhao, C.J. Xu, L. Zhang, Y. Yu, H.Z. Wang, Y.C. Lan, M.F. Roberts, J.H. Chuang, M.J. Naughton, Z.F. Ren, T.C. Chiles, A molecular-imprint nanosensor for ultrasensitive detection of proteins, Nat. Nanotechnol. 5 (2010) 597–601.
[17] D. Dechtrirat, N. Gajovic-Eichelmann, F.F. Bier, F.W. Scheller, Hybrid material for protein sensing based on electrosynthesized MIP on a mannose terminated selfassembled monolayer, Adv. Funct. Mater. 24 (2014) 2233–2239.
[18] T.M.A. Gronewold, Surface acoustic wave sensors in the bioanalytical field: recent trends and challenges, Anal. Chim. Acta 603 (2007) 119–128.
[19] K. Länge, B.E. Rapp, M. Rapp, Surface acoustic wave biosensors: a review, Anal. Bioanal. Chem. 391 (2008) 1509–1519.
[20] V.V. Losev, A.V. Medved, A.V. Roshchin, R.G. Kryshtal, B.I. Zapadinskii, I.D. Epinat'ev, I.V. Kumpanenko, An acoustic study of the selective absorption of vapors by microporous polymer films, Russ. J. Phys. Chem. B 3 (2009) 990–1003.
[21] W. Wen, S.T. He, S.Z. Li, M.H. Liu, P. Yong, Enhanced sensitivity of SAW gas sensor coated molecularly imprinted polymer incorporating high frequency stability oscillator, Sens. Actuators B Chem. 125 (2007) 422–427.
[22] R. Boroznjak, A. Tretjakov, V. Syritski, J. Reut, A. Öpik, Unpublished results, (2015).
[23] M. Bosserdt, J. Erdossy, G. Lautner, J. Witt, K. Kohler, N. Gajovic-Eichelmann, A. Yarman, G. Wittstock, F.W. Scheller, R.E. Gyurcsanyi, Microelectrospotting as a new method for electrosynthesis of surface-imprinted polymer microarrays for protein recognition, Biosens. Bioelectron. 73 (2015) 123–129.
[24] K.J. Jetzschmann, G. Jagerszki, D. Dechtrirat, A. Yarman, N. Gajovic-Eichelmann, H.D. Gilsing, B. Schulz, R.E. Gyurcsanyi, F.W. Scheller, Vectorially Imprinted Hybrid Nanofilm for Acetylcholinesterase Recognition, Adv. Funct. Mater. 25 (2015) 5178–5183.
[25] Y. Liu, L. Shen, From Langmuir kinetics to first- and second-order rate equations for adsorption, Langmuir ACS J. Surf. Coll. 24 (2008) 11625–11630.
[26] S. Lagergren, Zur theorie der sogenannten adsorption gelöster stoffe, Kungliga Svenska Vetenskapsakademiens, Handlingar 24 (1898) 1–39.
[27] W. Plazinski, W. Rudzinski, A. Plazinska, Theoretical models of sorption kinetics including a surface reaction mechanism: a review, Adv. Colloid Interfac. 152 (2009) 2–13.
[28] Y.S. Ho, Review of second-order models for adsorption systems, J. Hazard Mater. 136 (2006) 681–689.
[29] C.Y. Chen, C.H. Wang, A.H. Chen, Recognition of molecularly imprinted polymers for a quaternary alkaloid of berberine, Talanta 84 (2011) 1038–1046.
[30] K. da Mata, M.Z. Corazza, F.M. de Oliveira, A.L. de Toffoli, C.R.T. Tarley, A.B. Moreira, Synthesis and characterization of cross-linked molecularly imprinted polyacrylamide for the extraction/preconcentration of glyphosate and aminomethylphosphonic acid from water samples, React. Funct. Polym. 83 (2014) 76–83.
[31] Q.P. You, Y.P. Zhang, Q.W. Zhang, J.F. Guo, W.H. Huang, S.Y. Shi, X.Q. Chen, High-capacity thermo-responsive magnetic molecularly imprinted polymers for selective extraction of curcuminoids, J. Chromatogr. A 1354 (2014) 1–8.
[32] W. Rudzinski, W. Plazinski, On the applicability of the pseudo-second order equation to represent the kinetics of adsorption at solid/solution interfaces: a theoretical analysis based on the statistical rate theory, Adsorption 15 (2009) 181–192.
[33] R.J. Umpleby 2nd, S.C. Baxter, Y. Chen, R.N. Shah, K.D. Shimizu, Characterization of molecularly imprinted polymers with the Langmuir–Freundlich isotherm, Anal. Chem. 73 (2001) 4584–4591.
[34] A.M. Rampey, R.J. Umpleby, G.T. Rushton, J.C. Iseman, R.N. Shah, K.D. Shimizu, Characterization of the imprint effect and the influence of imprinting conditions on affinity, capacity, and heterogeneity in molecularly imprinted polymers using the Freundlich isotherm-affinity distribution analysis, Anal. Chem. 76 (2004) 1123–1133.